

A Population-Based Model of the Effects of Spinal Cord Stimulation on Pain Processing

Ariella Goldberg

Mentors: Sofia Piltz, Jennifer Crodelle, Victoria Booth

E-mail: acgoldberg19@amherst.edu

Abstract. Painful stimuli are processed in the dorsal horn, a region in the spinal cord where several types of fibers send information to groups of neurons. We modify a mathematical model of the behavior of the neuron populations in the dorsal horn circuit by adjusting parameters of fiber and neuron behavior, and use this to simulate the body's response to pain. In this way, we are able to qualitatively match experimental results observed in neurological studies. Our model incorporates Spinal Cord Stimulation (SCS), a procedure that often inhibits several types of pain. For example, SCS has been shown to be more effective in treating neuropathic pain, which results from damage to the nervous system, than nociceptive pain, which is more common and results from injury to the body [1]. With our model, we have found that we are able to capture the results of SCS, but further adjustment will be necessary to show that repeated SCS pulses yield a net decrease in pain.

1. Introduction

The dorsal horn area of the spinal cord serves as the body's primary pain-processing center, receiving sensory information from all regions of the body, and transmitting signals to several regions of the brain. Neurons located in the dorsal horn respond to information from afferent fibers¹, which react to painful and non-painful stimulus in peripheral organs like the skin (see Figure 1). Our model describes the firing rate of neuron populations in the dorsal horn circuit. We model the interactions between the excitatory, inhibitory and projection neuron populations, given their respective inputs from the $A\beta$, $A\delta$ and C fibers. The activity of excitatory and inhibitory neurons is crucial for the body's well-functioning detection of pain. When the body detects a painful stimulus, the activity of excitatory neurons outweighs the activity of inhibitory neurons, which alerts projection neurons into communicating the presence of pain to the brain. The neurons receive inputs from different types of afferent fibers based on their role in pain processing. The $A\delta$ and C fibers are nociceptive pain-detecting fibers, which stimulate excitatory and projection neurons. The $A\beta$ fibers respond to innocuous stimulation, and increase inhibitory and projection neuron activity. The primary motivation of our model is to investigate the impact of Spinal Cord Stimulation (SCS) on pain processing. SCS is a clinical treatment for chronic pain which uses implanted electrodes to stimulate $A\beta$ fibers in the dorsal columns [2]. The efficacy of this procedure remains unclear. Based on the gate-control theory of pain (1965), the non-noxious stimulation of $A\beta$ fibers upon SCS administration should suppress the body's

¹ In this paper, we will discuss the role of the three main groups of afferent fibers ($A\beta$, $A\delta$ and C), which are structures in the peripheral nervous system that transmit information from the bodily organs to the brain [6].

perception of painful sensation. However, there are different causes for painful sensation, and still research on whether SCS is effective in treating neuropathic (nerve damage-related) pain, or nociceptive (tissue damage-related) pain [1]. Our model displays the effect of SCS on ongoing, almost-painful “pinch” stimulus. We are interested in observing the impact of SCS on neuron population activity levels using a clear mathematical model.

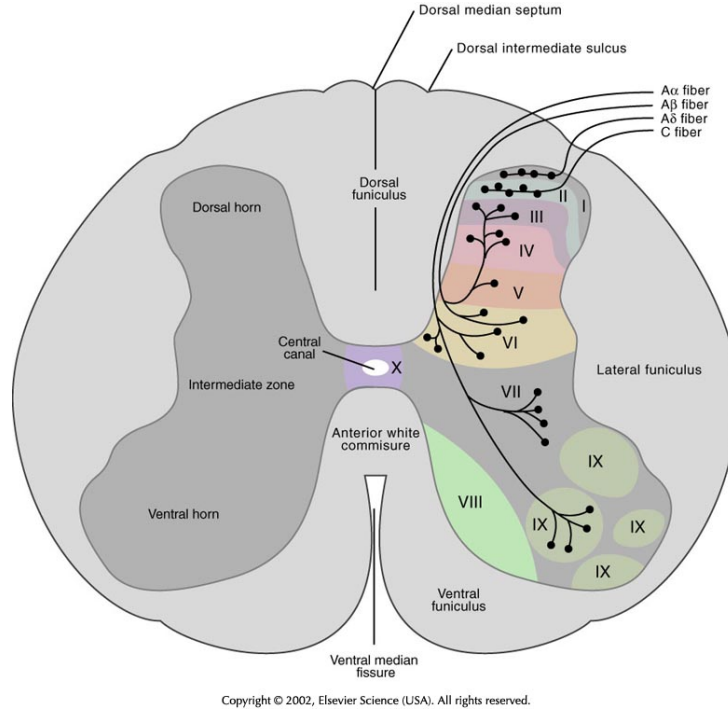


Figure 1. Spinal cord input from dorsal root ganglion. Adapted from Summers [3].

2. Methods

2.1. Model Equations

The following set of equations describes the average firing rate of each population of neurons in the dorsal horn:

$$\frac{df_I}{dt} = \frac{I_\infty(g_{A\beta I}f_{A\beta}(t)) - f_I}{\tau_I}, \quad (1)$$

$$\frac{df_E}{dt} = \frac{E_\infty(g_{CE}f_C(t) - g_{IE}f_I) - f_E}{\tau_E}, \quad (2)$$

$$\frac{dg_{NMDA}}{dt} = \frac{M_\infty(f_W)max_g - g_{NMDA}}{\tau_{NMDA}}, \quad (3)$$

$$\frac{df_W}{dt} = \frac{W_\infty(g_{A\beta W}f_{A\beta}(t) + g_{A\delta W}f_{A\delta}(t) + (g_{CW} + g_{NMDA})f_C(t) + g_{EW}f_E - g_{IW}f_I) - f_W}{\tau_W}. \quad (4)$$

The I_∞ , E_∞ and W_∞ terms represent the monotonic and increasing firing rate response functions of each neuron population. The weights, denoted g_{ij} , each have subscripts which

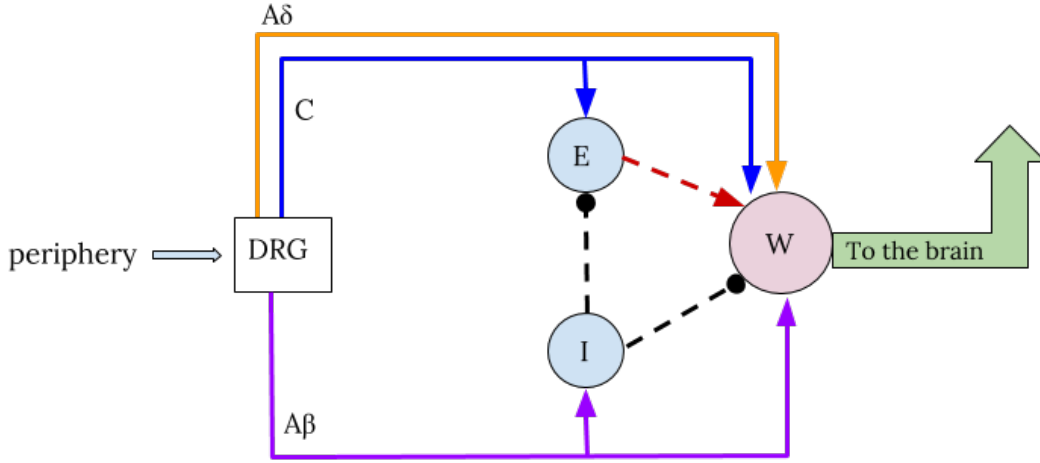


Figure 2. Diagram of our model for the dorsal horn circuit. The dorsal root ganglion (DRG) receives sensory information from periphery tissues and sends this input to the $A\beta$, $A\delta$ and C fiber populations (see Section 1). The bars directly connected from the DRG to the neuron populations are labeled according to fiber group. Solid arrows represent excitatory connections between fibers and neurons, while dotted arrows represent excitatory relationships between neuron populations. Dotted bars with circular ends indicate an inhibitory relationship between neuron populations. The $A\beta$ fiber connections are indicated in purple, the C fiber connections in blue, and the $A\delta$ fiber connections in orange. The neuron populations, consisting of excitatory (E), inhibitory (I) and projection (W) neurons, are labeled with colored circles. The excitatory neurons increase projection neuron activity, while the inhibitory neurons dampen projection neuron activity. The circuit terminates in the projection neurons, which send painful signals to the brain.

describe the direction of influence (e.g. $g_{A\beta W}$ denotes the impact of a change in $A\beta$ on W). The intrinsic time scale is represented by τ , where $\tau_W=1\text{ms}$, $\tau_E=10\text{ms}$, $\tau_{NMDA}=1\text{ms}$, and $\tau_I=20\text{ms}$. The $f_k(t)$ terms represent the functions of average firing rate of each k fiber population with respect to time. In addition, we have an equation representing the weight g_{NMDA} as a function of time (Equation 3). The weight g_{NMDA} refers to the strength of the C fiber influence on the projection neuron firing rate through NMDA receptors². We assume that this strength changes according to the projection neuron firing rate, and so we express the NMDA synaptic weight as a function of time. Within the confines of this research project, we did not experiment with changes in this variable, and so it will not require further discussion.

² NMDA receptors are neurotransmitter receptors located in the membrane of a neuron, which influence the potential of information transfer [5].

The average firing rate of the inhibitory neuron population (see Equation 1) is based upon the firing rate response function I_∞ , the activity of the A β fibers ($f_{A\beta}(t)$), and the time constant τ_I . Since the inhibitory neuron population receives input only from the A β fiber population (see Table 1), the $f_{A\beta}(t)$ fiber term is positive in Equation 1. Similarly, the weight $g_{A\beta I}=0.6$ (see Table 1) indicates the positive input of the A β fiber population activity on the inhibitory neuron average firing rate. We subtract the f_I term so to account for the previous timestep output (this step is consistent through all equations in this section).

The average firing rate of the excitatory neuron population (see Equation 2) takes positive input from the C fiber population (see Table 1), as is indicated by the weight g_{CE} multiplied by the $f_C(t)$ average firing rate term. We subtract $g_{IE}f_C(t)$ because the average firing rate of the inhibitory neuron population has a negative impact on the average firing rate of the excitatory neuron population.

The average firing rate of the projection neuron population (see Equation 4) takes positive input from the A β fiber population firing rate (indicated by the term $g_{A\beta W}f_{A\beta}(t)$), the A δ fiber population firing rate (indicated by the term $g_{A\delta W}f_{A\delta}(t)$), the C fiber population firing rate which includes an NMDA receptor connection strength (indicated by the term $(g_{CW} + g_{NMDA})f_C(t)$), and the excitatory neuron population firing rate (indicated by the term $g_{EW}f_E$). The projection neuron population average firing rate is decreased by the inhibitory neuron population average firing rate. We represent this by subtracting the term $g_{IW}f_I$. In the sections following, we will analyze the inputs to these model equations.

2.2. Equations for the Response Functions

The following equations describe the behavior of the neuron populations (see corresponding output in Figure 4):

$$W_\infty(x) = \max_W \frac{1}{2} \left(1 + \tanh \left(\frac{1}{\alpha_W} (x - \beta_W) \right) \right), \quad (5)$$

$$E_\infty(x) = \max_E \frac{1}{2} \left(1 + \tanh \left(\frac{1}{\alpha_E} (x - \beta_E) \right) \right), \quad (6)$$

$$I_\infty(x) = \max_I \frac{1}{2} \left(1 + \tanh \left(\frac{1}{\alpha_I} (x - \beta_I) \right) \right) + 1, \quad (7)$$

$$M_\infty(x) = \max_M \frac{1}{2} \left(1 + \tanh \left(\frac{1}{\alpha_M} (x - \beta_M) \right) \right). \quad (8)$$

We use hyperbolic tangent function to represent the firing rate response functions based on its qualitative comparison with experimental results, as one can see in Figure 3. The shape of the curve is determined by the parameter β , which is when the firing rate reaches half its maximum value; this value is equal to β_W , β_E and β_I for each population. The steepness of the curve's transition from non-firing to firing is given by $\frac{1}{\alpha_W}$, $\frac{1}{\alpha_E}$ and $\frac{1}{\alpha_I}$. The terms $\max_W=50$, $\max_E=60$, and $\max_I=80$ represent the maximum firing rates for the projection, excitatory and inhibitory neuron populations respectively. Similarly, the term $\max_M=2.0$ indicates the maximum strength of the NMDA receptor pathway. We account for our assumption that the baseline firing rate of inhibitory neurons, even without stimulus, is greater than 0 by adding 1 to Equation 7 [4].

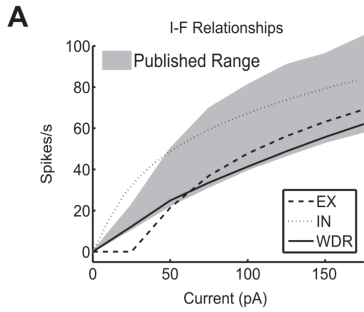


Figure 3. Previous experimental data provides evidence that the tangent functions are well-representative of the shape of the response curves. Compare with Figure 4. Adapted from Zhang et al. *J. Neurophysiol.* 2014 [4].

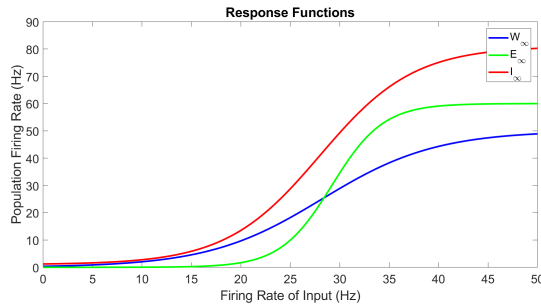


Figure 4. Model of how the firing rate of a population depends on the firing rate of the output from the $A\beta$, $A\delta$, and C fibers. Previous experimental data provides evidence that the tangent functions are well-representative of the shape of the response curves [4].

2.3. Generating the fiber activity

The $f_{A\beta}$, $f_{A\delta}$ and f_C terms in the model equations denote the activity of the $A\beta$, $A\delta$ and C fiber populations with respect to time. We assume that the $A\beta$ fiber population is 300, the $A\delta$ fiber population is 90, and the C fiber population is 820. We simulate 2000 milliseconds of neuron activity, where the first 300ms are base level activity for all three fibers; we assume a baseline firing rate of 1Hz, without stimulus or SCS, for all three fiber populations (see Figure 5). Upon “pinch” stimulus, the $A\beta$ and $A\delta$ average firing rates increase to 9Hz and the C fiber firing rate increases to 2.5Hz. We organize the activity of each of the fiber populations in matrices, where the number of rows corresponds to the number of fibers, while the number of columns is equal to the number of milliseconds in the simulation. If a fiber spikes at a certain millisecond, a 1 is placed in the cell corresponding to the appropriate fiber at that time. We use a Poisson process to generate the spike times of each fiber, then convert this output to the instantaneous firing rate in each of the fiber groups. Increasing the firing rate in the fiber groups results in a higher probability that each fiber will spike per millisecond; therefore, during an almost-painful “pinch” stimulus, $A\beta$ fibers have higher activity than during a baseline non-“pinch” state. We create a smooth average firing rate by using a moving average over the number of spikes. We run the simulation over 20 realizations by generating 20 random seeds for the Poisson process. We then take the average over all realizations.

Each type of fiber responds to the “pinch” at a different time. Beginning at 300ms, the firing rate of $A\beta$, $A\delta$ and C fibers increases to indicate that they have received stimulus input from the dorsal root ganglion (see Figure 5). $A\beta$ fibers, because of their thick myelination and rapid conductance, respond first at 300ms. At 320ms, the medium diameter, myelinated $A\delta$ fibers respond to the stimulus (see Figure 5). Finally, at 390ms the small diameter, unmyelinated C fibers respond to the “pinch.” The heightened activity of the fibers increases the inputs to the neuron populations, which consequently fire at a heightened rate (see Figure 5 and Figure 8).

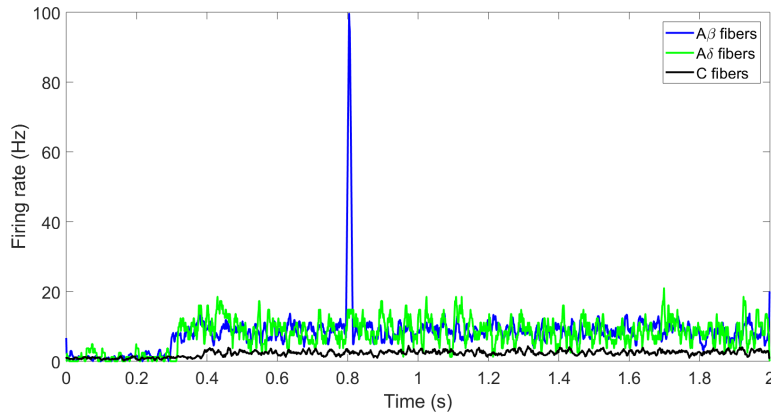


Figure 5. The firing rate of the fibers based on the model inputs in Table 1. We see the reaction to the SCS pulse in the $A\beta$ fibers between 0.8 and 0.9 seconds.

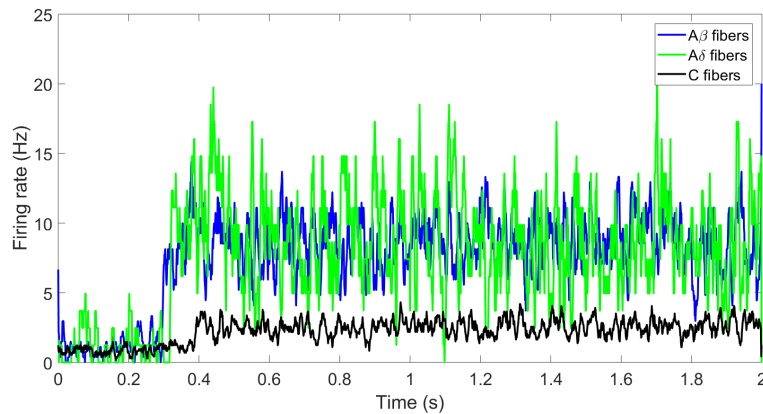


Figure 6. The firing rate of the fibers based on the model inputs in Table 1, without the SCS implemented. Compare with Figure 5.

To introduce SCS to our model, we increase the average firing rate of the $A\beta$ fibers for the duration of SCS effect. In accordance with experimental results which describe the action potential duration for $A\beta$ fibers as about 5ms [2], we assume that the observed reaction to SCS in the $A\beta$ fiber population occurs within a response window of 10ms with respect to the SCS pulse. This is the $A\beta$ response to a single pulse of SCS, during which we expect a certain percentage of the $A\beta$ fibers to spike exactly once. The percentage of the $A\beta$ fibers activated depends on the strength of the SCS administered. Since we cannot take into account the dosage of the SCS applied (see Section 3), we model SCS strength as a percentage of $A\beta$ fibers which are impacted by SCS (see Figure 9). In order to activate a certain percentage of the $A\beta$ population within the 10ms response window, we randomly distribute a single spike for each activated $A\beta$ fiber within 10ms after the start of SCS, which is 800ms in our model. To do this, we generate a single random number, call it p , between 0 and 10 for each $A\beta$ fiber activated, and place a 1 (a spike) at the time index $800 + p$ for the relevant fiber. Consequently, the average firing rate of the $A\beta$ fiber population increases from 9Hz to about 100Hz in response to the SCS.

Populations	Weights
$g_{A\beta W}$	0.8
$g_{A\delta W}$	1.8
g_{CW}	0.5
g_{EW}	1
g_{IW}	1
g_{CE}	5
g_{IE}	0.4
$g_{\beta I}$	0.6

Table 1. Weights between populations.

2.4. Adjusting the Weights Between Populations

In order to choose the set of weights between populations (see Table 1), we tested small changes of each weight until we found firing rate behavior that matched published experimental results [2][4]. We first adapted a figure from our previous model, which has a shorter simulation time and different firing rates for the $A\beta$, $A\delta$ and C fibers. We extended the simulation to 2000ms and changed the baseline and “pinch” firing rates for each fiber population in order to compare with parameters from previous experiments, namely Zhang et al. [4]. According to experimental results, the threshold of pain, or the minimum firing rate for the body to process a stimulus as painful, is when the projection neurons fire at 25Hz [1]. We decided to adjust our model until the baseline firing rate of projection neurons is just below painful, and would most likely produce the sensation of a “natural pinch.” In order to do this, we needed to achieve a balance among the weights so that the resulting projection neuron firing rate, during an almost-painful natural “pinch” stimulus, would have an average of about 20Hz—near, but not exceeding 25Hz. Likewise, the excitatory and inhibitory neuron populations also needed to reflect an appropriate reaction to this stimulus. We would expect the excitatory neuron population average firing rate to increase upon “pinch” stimulus, and in turn the inhibitory neuron population average firing rate to increase [4].

3. Results

3.1. Model output in response to a painful stimulus

Our model successfully captures the effects of the dorsal horn circuit output during a natural “pinch” stimulus, as well as the effects of SCS (see Figure 8 for the model output with SCS). With our current set of weights (see Table 1), the average firing rate of projection neurons in our model during the “pinch” is 16.72Hz (see Figure 8). We ran the simulation for 20 realizations (see Section 2.3). Under experimental conditions, we would expect the average projection neuron firing rate to be slightly higher during a natural “pinch”: about 20Hz. However, we faced certain challenges in adjusting the weights (see Section 4), and this value is the result of the most functional weights for our model. Since our average firing rate of the projection neurons in response to “pinch” stimulus remains within proximity of the 20Hz ideal projection neuron firing rate, we decided to push forward and investigate other abilities of the model.

3.2. Modeling the Effects of Spinal Cord Stimulation

In order to simulate the SCS, we cause a specific percentage of the $A\beta$ fiber population to spike exactly once in response to one pulse of the SCS (see Section 2.3). In the literature, it is

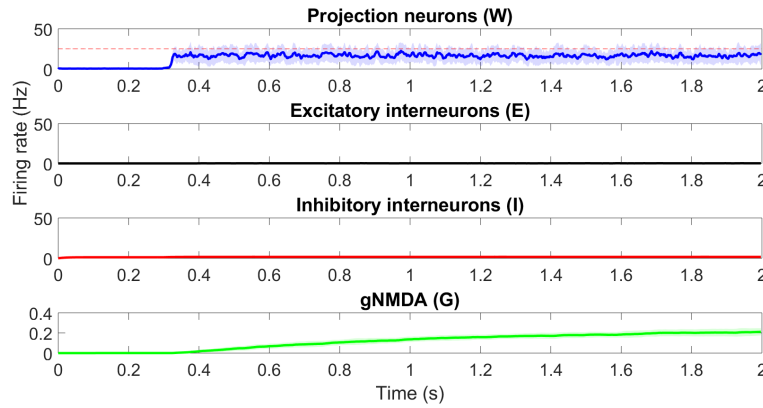


Figure 7. Average firing rate of the neuron populations with the “natural pinch” stimulus starting at 300ms (0.3s) and persisting until 2000ms (2.0s). Compare with Figure 8 for an example of the model behavior with the SCS simulated.

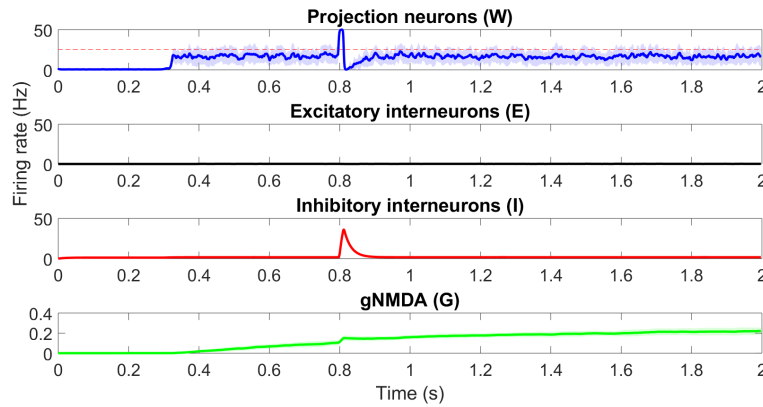


Figure 8. Response to a single pulse of the SCS at 800ms (0.8s) in the neuron population average firing rates, as well as the NMDA synaptic weight. This represents a high strength of the SCS, with all $A\beta$ fibers activated by the SCS. The “natural pinch” begins at 300ms (0.3s) and sustained until the end of the simulation. The projection neuron average firing rate decreases from an average of 16.72Hz during the “pinch” to an average of 3.92Hz after the initial spike (measured from 815ms to 850ms). We see an initial spike in projection neurons because of the weight from the $A\beta$ fibers to the projection neurons (see Table 1). After the 10ms when we see the effects of the SCS, the projection neuron average firing rate returns to “pinch” levels.

common to refer to the SCS strength in terms of amount of current applied [1]. Initially, we attempted to simulate the SCS by attributing a higher firing rate to the $A\beta$ fibers during the time of expected response to the SCS pulse (e.g. 60Hz in comparison to the “natural pinch” response 9Hz). However, this did not guarantee that every $A\beta$ fiber would spike, and we were mainly concerned with capturing the synchronization of $A\beta$ fiber spike times in response to the SCS pulse. Likewise, 60Hz was not the SCS pulse activity, but instead the frequency at which it was administered in various experiments [1]. We then revised our approach, and automated the code to place 1s within the spike matrix of the $A\beta$ fiber population, thereby guaranteeing that the desired amount of $A\beta$ fibers would spike exactly once within the window of time that

we expect to see the impact of the SCS pulse.

Our new method toward simulating the SCS allows for the visualization of different “strengths” of the SCS pulse; for instance, the SCS pulse that causes 100 percent of the $A\beta$ fibers to spike is “stronger” than the pulse that causes 50 percent of the $A\beta$ fibers to spike. Figure 9 illustrates the average firing rate of the projection neurons in terms of percent of the “natural pinch” firing rate, when different percentages of the $A\beta$ fiber population are activated by the pulse. Our model is sensitive to changes in the number of $A\beta$ fibers activated. It is clear that larger percentages of $A\beta$ fibers activated causes significant inhibition of the projection neuron response to painful stimulus.

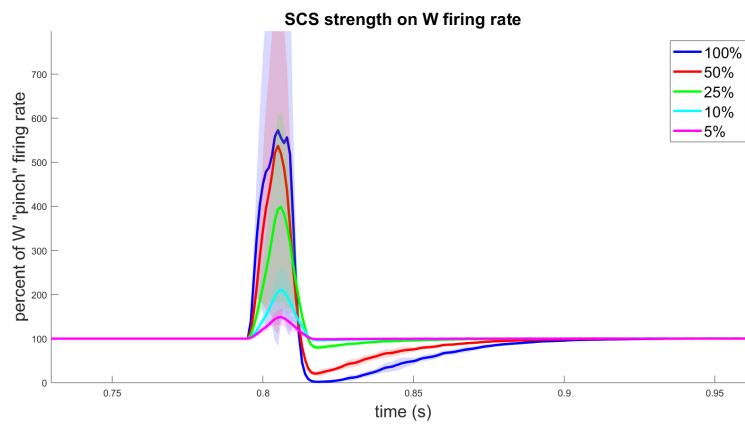


Figure 9. Average firing rate of the projection neuron population in response to a single pulse of the SCS. Calculated in terms of percent of baseline (“natural pinch”) firing rate. Demonstrates five different “strengths” of the SCS, in terms of percentage of $A\beta$ fiber population activated by the SCS (see Section 4). At 500ms (0.5s) in the simulation, we see the projection neuron firing rate in response to the “natural pinch” stimulus. At 800ms (0.8s), the SCS is simulated, and the reaction takes place for a subsequent 10ms duration. The 100 percent strength of the SCS causes complete dampening of the projection neuron population average firing rate in response to the simulated “natural pinch.”

We are interested in testing the effectiveness of SCS by investigating whether the SCS pulse in our model causes a net decrease in the projection neuron firing rate during a painful stimulus. Our model displays an inhibition of the projection neuron firing rate in response to SCS, but only after an initial projection neuron spike. This initial increase is due to the weight from the $A\beta$ fiber population to the projection neurons (see Table 1). Although the $A\beta$ fibers also increase the firing rate of the inhibitory neuron population, which consequently dampen projection neuron activity, this intermediate step delays the inhibition of projection neuron firing rate. In effect, we see the excitatory influence of the $A\beta$ fiber weight on the projection neuron population firing rate before we see the effects of the $A\beta$ fiber weight on the inhibitory neuron population firing rate; an increase in the $A\beta$ fiber firing rate immediately increases the projection neuron firing rate (through the weight g_{ABW}) and the inhibitory neuron firing rate (through the weight g_{ABI}), and so there is a momentary spike in the projection neuron population activity before it is dampened by the inhibitory neuron population activity through the weight g_{IW} (see Figure 1). With suitable binning of time and distributing the spikes in the projection neuron population average firing rate, we are able to minimize the appearance of this initial spike (see Figure 11); previous literature showcases similar tactics [1]. However, the initial spike in projection

neuron firing rate becomes problematic when we attempt to use our model to replicate other experimental scenarios. This issue becomes relevant when we model the implementation of multiple pulses of the SCS in our model (see Figure 12). Although our model is capable of simulating this process, the initial spikes in the projection neuron population average firing rate are too extreme for the subsequent decreases to overcome over the sum of several pulses. The result is a visible net increase in percent of projection neuron firing rate. For this reason, we are unable to recreate the exact results from Zhang et al., although we are able to capture a similar process [4].

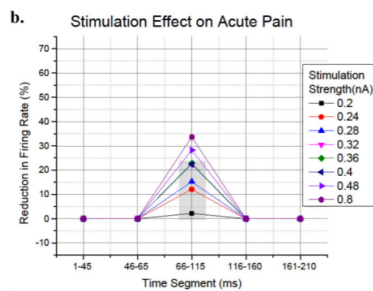


Figure 10. The effect of SCS on acute pain. Adapted from Arle et al (2014).

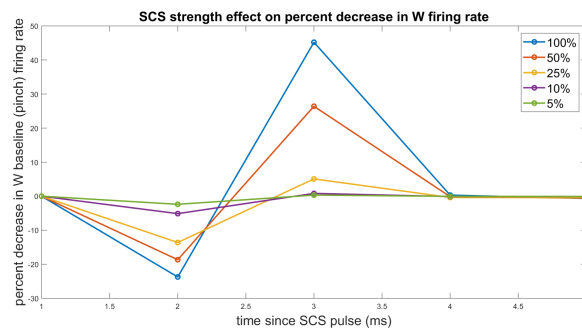


Figure 11. Comparison of different strengths of SCS (in terms of percentage of the $A\beta$ fiber population activated by a single SCS pulse) on the percent decrease in projection neuron population average firing rate. The sum of the time bins is equal to a net decrease of 12.61.

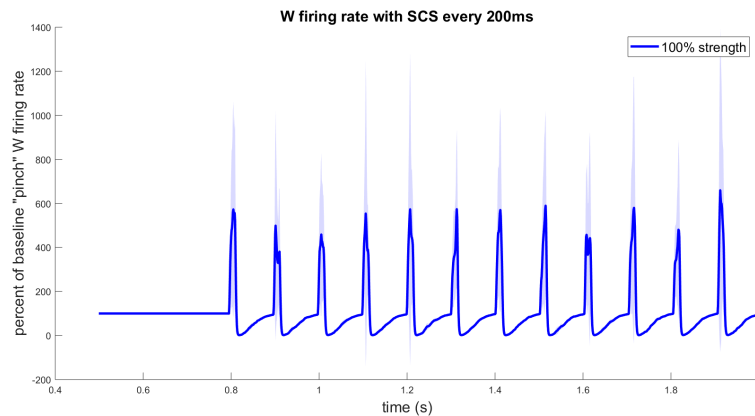


Figure 12. Projection neuron population average firing rate as a percentage of baseline (“natural pinch”) firing rate. Simulation of many SCS pulses, administered every 200ms with the first pulse at 800ms (0.8s). The increase in projection neuron firing rate at the onset of each SCS pulse in response to the sudden increase in firing rate of the $A\beta$ fiber population, causes there to be a net increase in the average firing rate of the projection neuron population in response to multiple SCS pulses.

4. Discussion

Our neuron population model successfully simulates the body’s reaction to painful stimulus using computational strategies. In addition, our model captures the dorsal horn circuit response to SCS; although we are in the process of improving the projection neuron initial response to the SCS, the population firing rate does decrease using our model equations and weights. The model is easy to use and adaptable to changes in the population weights, the duration of the SCS effects, the strength of the SCS simulated, and many other parameters. In comparison to neurological models, our model provides an accessible, mathematically clear and manipulable simulation of the dorsal horn’s pain processing function. Our model could potentially be useful in predicting the SCS strength that is effective for producing a net decrease in projection neuron firing rate; this could influence decisions in research settings, such as where to effectively place electrodes in order to target a certain percentage of the $A\beta$ fiber populations.

However, we also came across challenges in producing our model, and we consider ways to improve it. While experimenting with the weights, we found that some responses were easier to generate than others (see Section 2.4). For instance, we found it relatively easy to influence the projection neuron average firing rate with small changes in the $g_{A\beta W}$ and $g_{A\delta W}$ weights. Similarly, the duration of initial projection neuron spike at the onset of the SCS is sensitive to the $g_{A\beta I}$ weight. On the other hand, within our model it is difficult to elevate the excitatory neuron firing rate. The excitatory neuron population average firing rate is about 0.006 for the entire simulation (see Figure 8). Even when the “pinch” is administered, we do not see a visible change in the average firing rate. This is likely because the excitatory neuron population receives input only from the C fiber population (see Table 1, Figure 2), which have a “pinch” stimulation firing rate of only 2.5Hz. This means that the excitatory neuron population receives very little input, especially in comparison to the other neuron populations. We found that we barely see any excitatory neuron population activity until we set the weight from the C fiber population to the excitatory neurons to at least $g_{CE}=8$ or $g_{CE}=9$ (the ideal weight is $g_{CE}=11$). The issue with raising this weight so high is that it is out of scale with the other weights in the model (see Table 1). We attempted to increase all of the weights to be in scale with a high C-to-E weight. However, this option made it difficult to dampen excitatory neuron activity under realistic circumstances, such as when inhibitory neurons become activated. We decided to settle with our current set of weights, with the $g_{CE}=5$, which is about as high as it can go without being out of scale with the other weights. There is little known information about the weights between the afferent fibers and the projection neurons [1]; this is why we based our approach to finding the appropriate set of weights by comparing the resulting output with qualitative experimental results. Perhaps this set of weights could be modified slightly to encapsulate the realistic behavior of the excitatory neuron population with a painful stimulus.

One future adaptation for our model could be to adjust the set of weights so that the projection neuron average firing rate during the simulated “natural pinch” is closer to 25Hz. We also aim to improve the model of many SCS pulses (see Figure 12) so that the simulation yields a net decrease in percent of average projection neuron firing rate. To accomplish this, we would like to minimize the initial spike in projection neuron firing rate in response to the SCS pulse.

Overall, we have found that Spinal Cord Stimulation is an effective treatment for inhibiting prolonged, dull pain. However, it depends on the strength of the SCS applied, and the way in which the projection neuron population reacts to the initial spike in the $A\beta$ fiber firing rate.

Acknowledgments

I would like to express my gratitude to my mentors Victoria Booth, Sofia Piltz, and Jennifer Crodelle whose constant support and guidance was inherent to the success of this research project and my growth as a math student. I would also like to thank the University of Michigan

REU program and the National Science Foundation for providing funding for our work.

References

- [1] J.E. Arle, K.W. Carlson, L. Mei, N. Iftimia, J.L. Shils, Mechanism of Dorsal Column Stimulation to Treat Neuropathic but not Nociceptive Pain: Analysis With a Computational Model, *Neuromodulation*, **17**, 642-655 (2014).
- [2] J.P. Miller, S. Eldabe, E. Buchser, L.M. Johaneck, Y. Guan, B. Linderoth, Parameters of Spinal Cord Stimulation and Their Role in Electrical Charge Delivery: A Review. *Neuromodulation*, **19**, 373-384 (2016).
- [3] Summers, C., Behavioral Neuroscience: Fear Conditioning. <http://usdbiology.com/cliff/Courses/Behavioral%20Neuroscience/Fear/FCfigs/FCcirpics.html> (Accessed July 21, 2018).
- [4] T.C. Zhang, J.J. Janik, W.M. Grill, Modeling effects of spinal cord stimulation on wide-dynamic range dorsal horn neurons: influence of stimulation frequency and GABAergic inhibition, *J. Neurophysiol*, **112**, 552-567 (2014).
- [5] 2017: NMDA Receptor - Definition, Function, Structure, Quiz. <https://biologydictionary.net/nmda-receptor/>. Accessed July 30, 2018.
- [6] 2017: Peripheral Nervous System - Definition, Function & Example. <https://biologydictionary.net/peripheral-nervous-system/>. Accessed July 30, 2018.